Travelling Wave Positron Injector Linac for TESLA

K.Floettmann[1], K.Jin[2], S.H.Wang[3] and F.Zhou[3]

[1] DESY, MPY, Notkestr.85, 22603 Hamburg, Germany
[2] NSRL, University of Science and Technology of China, Hefei 230029, China
[3] Institute of High Energy Physics (IHEP), Beijing 100039, China

Abstract

A modified cup-like TW accelerating structure for the TESLA Positron Pre-Accelerator (PPA) has been designed by optimizing the structure geometry and by changing the iris thickness cell-by-cell in a section. This structure has a high shunt-impedance and a large iris radius to meet the requirements of high gradient and large transverse acceptance. The beam dynamics in the structure with the optimum solenoid focusing field have been studied, including the space-charge and beam-loading effects. A satisfactory positron beam transmission and the beam performance at the PPA output have been obtained.

1 Introduction

TESLA will use the spent electron beam (250 GeV, after collision at the IP) to produce a positron beam, by passing the spent electron beam through a wiggler to produce photons, which will hit a thin target to yield the positrons[1]. This positron source has the advantages of having a higher positron yield and a better positron beam performance at the target compared with the conventional concept of aiming high energy electrons onto a thick target[2].

Due to the large transverse momentum and emittance of the positron beam at the target, an Adiabatic Matching Device (AMD) had been designed[3], which immediately follows the target to provide the adiabatically-varying longitudinal magnetic field and to realize a phase-space transformation. The designed magnetic field Bz is varied along the axis z as

$$B_z = \frac{B_i}{1+gz} \tag{1}$$

where $B_i = 6.0T$ is the initial magnetic field at the AMD input and $g = 30m^{-1}$ is the taper parameter.

Our task in this paper is to design a Positron Pre-Accelerator (PPA) which will capture the positrons immediately after the AMD and accelerate them to about 250 MeV using a normal conducting, TW L-band structure. Following the PPA there is a Positron Booster Accelerator (PBA) which further accelerates the positrons up to about 3 GeV by using the TESLA superconducting L-band structure. The PBA will be the injector of the positron Damping Ring (DR). The positron chain of the target, AMD, PPA, PBA and DR is shown in Figure 1.

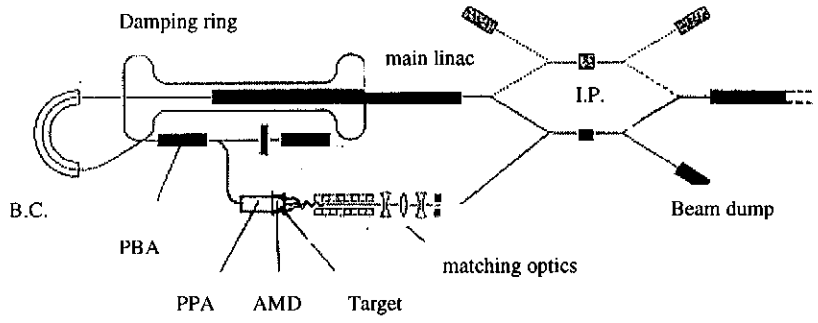

Fig.1 Sketch of the Positron Source, PPA, PBA and DR layout

2 Positron Beam Performances at the PPA Input and Output

2.1 At the PPA input (AMD output) the positron beam has the following performance:

- Large electric charge. The number of positrons per rf pulse $Ne^+/pulse > 2.8\times10^{14}$. The parasitic electron yield at the target is about a factor of 1.65 higher than the positrons yield, due to the ionization. These electrons are overlapped with positrons in the same space at the PPA input.
- Small spatial spot of about 10 mm, but with a large transverse momentum (Px/Pz, Py/Pz > 0.05) and large normalized emittance ($>5.0\times10^{-2}$ m).
- Large energy spread of 2 MeV-60 MeV. The energy domain is 5 MeV-25 MeV and the average energy of the positron beam is about 15 MeV.
- Large longitudinal phase spread. The positron bunch length is about ± 20 ps, or say 6-7 mm (about ± 10 degrees in L-band RF phase).
- The time structure of the positron beam[4]:

  Beam pulse length = 800 μ s.
  Pulse repetition rate =5 Hz and 4 Hz for the TESLA versions of Standard-500 and Reduced vertical emittance (ε_y)-500, respectively.
  Bunches/pulse= 1130 (Standard-500), 2260 (Reduced ε_y -500).
  Positrons/bunch = 2.48×10^{11} (Standard-500), 1.24×10^{11} (Reduced ε_y -500).
  Bunch spacing = 708 ns (Standard-500), 354 ns (Reduced ε_y -500).

The transverse and longitudinal beam performance at the PPA input are shown in Figure 2.

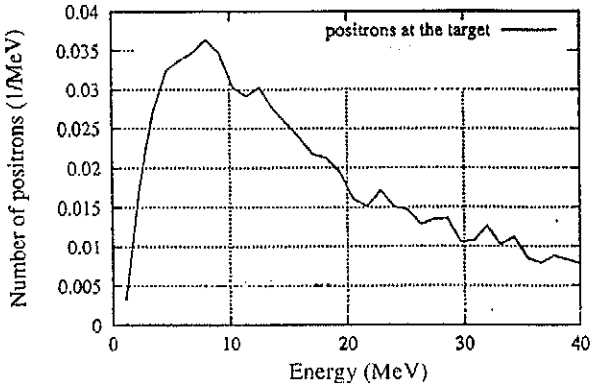

(a)

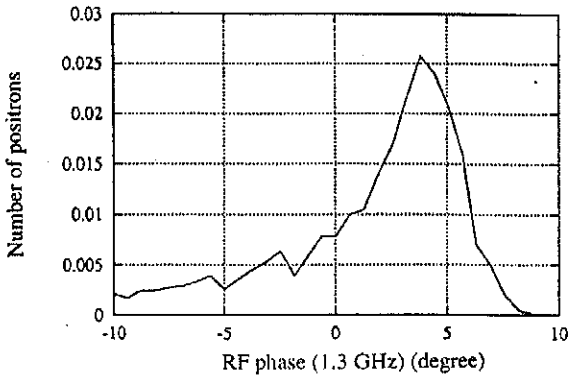

(b)

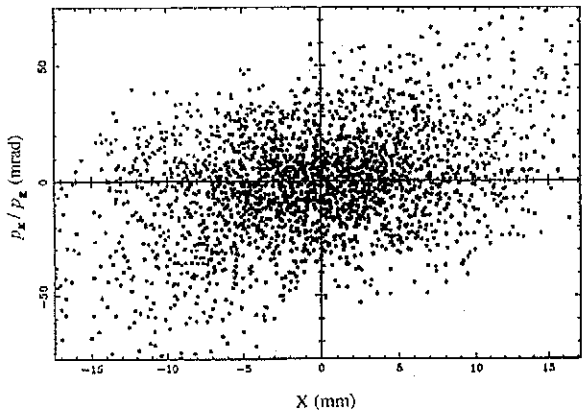

(c)

(a): Energy spectrum

(b): Phase spectrum

(c): Transverse phase space

Fig.2 The positron beam performance at PPA input

2.2 The required positron beam performance at the PPA output is:

- Positrons/pulse at the PPA output should be a factor of 2.5 larger than the design number at the IP, so that the design positrons/pulse in the damping ring will be a factor of about 2.0 larger than the one at the IP for a safe margin. It means that at the PPA output, the positrons/pulse = 1.028×10^{14}.

- The transverse beam emittance should be less than the DR acceptance of 4.8×10^{-2} m (normalized and 100% particles).

- The beam energy spread and phase spread required by the DR (at an energy of 3.2 GeV) are about $\pm 1\%$ and ± 7.5 degrees respectively[5]. This implies that the energy spread at the PPA output (250 MeV) should be approximately $\leq \pm 6.5\%$, which will be mentioned later.

3 Accelerating Structure

3.1 Technical Requirements for the PPA Accelerating Structure

Due to the special beam performance at the PPA input as mentioned above, it is clear that the PPA structure should:

- be normal conducting, which would be acceptable for the loss of a large amount of particles in the structure.
- work at low frequency, L-band (1.3 GHz), to have a large transverse acceptance which is composed by a solenoid field Bz and a large iris radius of the structure.
- have a high gradient, 12 MV/m-20 MV/m, to accelerate the positrons to relativistic energy as quickly as possible to minimize the bunch lengthening due to the solenoid field.
- have a high shunt-impedance, to lower the power loss and pulse heating due to the long pulse length (803 μ s), high gradient and high duty cycle (0.4%).

3.2 A Modified Cup-like Disc-Loaded Structure

A constant gradient structure with $2\pi/3$ operating mode was chosen for the structure to have a uniform power dissipation along the structure and a high accelerating efficiency.

Given the frequency, f_0 = 1.3 GHz, in order to have a reasonable shunt impedance (Zs), iris radius (a) and accelerating section length (Ls), one has to choose an important parameter, the attenuation constant τ_0, which defines the ratio of the output and the input power of the structure:

$$P_{out} = P_{in} \cdot e^{-2\tau_0} \tag{2}$$

and determines the power loss per unit length:

$$\frac{dp}{dz} = \frac{P_{in}}{L_s} \cdot (1 - e^{-2\tau_0}) \tag{3}$$

It is clear that the larger τ_0, the smaller the output power and hence the higher the power ratio. On the other hand, a smaller τ_0 gives a larger group velocity (V_g) of the structure and hence gives a larger iris radius ($V_g \propto a^4$) and a larger transverse acceptance. τ_0 = 0.55 nepers, which is a good compromise as will be seen later.

We started with a " cup-like " cell structure as used in the SBLC design[6], which has the advantages of precise manufacturing and high shunt-impedance, but modified it by changing the iris thickness cell-by-cell in each section to have both a high shunt-impedance and a large iris radius.

In a second step, we modified the structure so that each cell consists of "two half-cups", as shown in Figure 3. There are two outer-curves with radius R_b for each iris to further increase the shunt-impedance and hence, combined with changing the iris thickness cell-by-cell, to obtain a larger iris radius. The optimum cell geometry and its EM performance, calculated with MAFIA-code [7], are listed in Table 1.

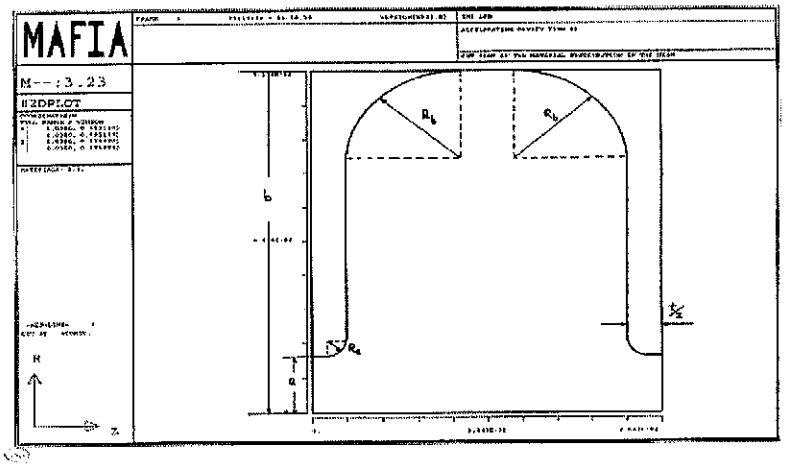

Fig.3 A modified cup-like disc-loaded structure

Table 1. The optimum geometry and its EM Performance

Nr.	a (mm)	b (mm)	t (mm)	Vg/c	Q	Zs ($M\Omega/m$)
01	17.612	93.188	12.00	0.00301	2.259E+04	51.20
02	17.486	93.182	12.15	0.00287	2.256E+04	51.20
03	17.360	93.176	12.30	0.00273	2.252E+04	51.19
04	17.234	93.170	12.45	0.00259	2.249E+04	51.18
05	17.107	93.165	12.60	0.00247	2.246E+04	51.18
06	16.981	93.160	12.75	0.00234	2.242E+04	51.14
07	16.855	93.156	12.90	0.00223	2.239E+04	51.14
08	16.729	93.152	13.05	0.00211	2.236E+04	51.14
09	16.603	93.148	13.20	0.00200	2.232E+04	51.10
10	16.477	93.144	13.35	0.00190	2.229E+04	51.09
11	16.351	93.140	13.50	0.00180	2.226E+04	51.07
12	16.224	93.137	13.65	0.00170	2.222E+04	51.03
13	16.098	93.134	13.80	0.00161	2.219E+04	51.02
14	15.972	93.131	13.95	0.00152	2.215E+04	50.98
15	15.846	93.129	14.10	0.00144	2.212E+04	50.95
16	15.720	93.127	14.25	0.00135	2.209E+04	50.93
17	15.594	93.125	14.40	0.00128	2.205E+04	50.89
18	15.467	93.123	14.55	0.00120	2.202E+04	50.86
19	15.341	93.121	14.70	0.00113	2.198E+04	50.81
20	15.215	93.120	14.85	0.00107	2.195E+04	50.79
21	15.089	93.119	15.00	0.00100	2.191E+04	50.79

In each cell $R_b = 25$ mm and $R_a = 4.75$ mm.

The advantages of the designed structure are summarized as follows:

- It is a constant gradient structure and also an almost constant impedance structure.
- It has a high shunt-impedance $Z_s > 50\,\mathrm{M}\Omega/\mathrm{m}$.
- It has a large iris diameter of 35.2 mm-30.2 mm.
- It has a thick iris of 12 mm-15 mm, so that the cooling channel can be directly passed through the inside of the iris, to have a high cooling efficiency. This is very important in the case of the PPA due to its high gradient and high duty cycle.
- The maximum surface electric field (at the radius R_a) in a cell is a factor of 1.98 higher than the averaged longitudinal electric field on the axis . That is acceptable to avoid RF breakdown.

3.3 Section Length and RF Power Supply

Taking an accelerating gradient of 12 MV/m and the shunt-impedance of $50\,\mathrm{M}\Omega/\mathrm{m}$, and if we choose the section length to be Ls = 7λ = 1.61427 m, then:

- Each section consists of 21 cells. The average energy gain of the positron beam per section is about 19.4 MeV, the pulse RF power for the structure is about 6.97 MW per section.
- Having 12 sections for the PPA, offers a final average energy of the positron beam at the PPA output of about 250 MeV, in which the initial average beam energy of 15 MeV at the PPA input is included.
- The beam power extracted from the structure is about 1.21 MW for the first section, which includes the positron and the parasitic electron beams. About 63% of the positrons and electrons will be lost (even more for electrons) in the first section and then the beam currents will be constant in the following sections. Therefore the beam power extracted from each of the following sections is about 0.65 MW. Hence the total power needed for the first section is about 8.18 MW and about 7.62 MW for each of other sections.
- Each section is powered by a klystron of 10 MW output, so that one has 18%-24% rf in reserve for beam loading compensations.
- The RF filling time into the sections is about $3.0\,\mu$ s, with Q-value of about 21500-22250 and attenuation constant of 0.55 nepers.
- The output RF power from each section at its end is about 33% of the input power, which can be absorbed by an absorber installed at the end of each section.
- The average power dissipation per unit length is about 17.3 kW/m and 13.8 kW/m for the TESLA versions of Standard-500 and Reduced ε_y-500 respectively, which are at the same level as the RF power dissipation of the cavities in some storage rings. Therefore it has no principle difficulties in the cooling system design.

3.4 Pulse Heating

If the pulse heating is higher than its safe value, the pulse mechanical stresses in the heated thin surface will cause a cyclic fatigue and the destruction of the structure within a limited period of time. In case of the PPA, due to its very long pulse length (803 μ s), the pulse heating has been of concern.

The estimated pulse heating is given by P.B.Wilson[8] as follows:

$$\Delta T = \frac{R_s}{K} \cdot (\frac{D\tau_p}{P_i})^{1/2} \cdot (\frac{E_0}{Z_h})^2 \qquad (4)$$

Where ΔT is the temperature rise caused by the pulse heating, Rs is the surface resistance (= $9.42\times10^{-3}\Omega$ for 1.3 GHz), K is the thermal conductivity ($=3.95W/cm/^0C$ for copper), D is the thermal diffusibility ($=1.15cm^2/\sec$, for copper), τ_p is the RF pulse length (= 803 μ s), E_0 is the accelerating gradient (=12 MV/m) and Z_h is the impedance defined by E_0/H_s, with H_s = 2070 A/m which is the maximum magnetic field obtained from a SUPERFISH calculation for the PPA structure. Hence the temperature rise due to pulse heating is about 2.53 ^{0}C which is much less than the safe value of 110 ^{0}C. So there will be no problem with pulse heating at the PPA.

4 Beam Dynamics in the PPA

The beam dynamics in the PPA with a TW structure has been studied analytically and by beam simulations with the PARMELA-code[9] as well.

4.1 Choice of the " synchronous phase "

Due to the large energy spread and the phase spread of the input beam, for the PPA beam dynamics studies, we first have to define the " optimum synchronous phase" by shifting the RF phase to obtain an optimum effective acceleration (max. energy gain), an optimum transmission and a reasonable beam performance, including the transverse emittance, energy spread and phase spread for most particles at the PPA output. In the primary calculations, E_0=12 MV/m and Bz=0.32 T were used. The selection of the Bz value will be explained later. The space charge and beam loading effects were neglected to begin which will also be discussed later.

Table 2. Beam performances with varying accelerating phase

Tr-wave Phase (degree)	Particle Transmission	Average Energy (MeV)	$\varepsilon_{n,x,rms}$ ($\times10^{-3}$m)	$\varepsilon_{n,y,rms}$ ($\times10^{-3}$m)	Energy Spread (rms)
0	21.5%	247.02	2.46	2.57	10.86%
-2	21.5%	247.78	2.47	2.53	10.57%
-4	21.5%	247.77	2.50	2.50	10.41%
-6	21.5%	247.71	2.50	2.50	10.22%

Table 2 lists the beam performance with different accelerating phase angles, obtained by the beam simulations with PARMELA. From this table one can see that the "optimum phase angle" in the PPA has a range of a few degrees, due to the large input energy spread and phase spread.

4.2 Choice of the Solenoid Magnetic Field

As we have mentioned in section 1.2, the number of positrons per pulse at the PPA output would be a factor of 2.5 higher than the one at the IP. If we define the beam transmission from the target to the PPA output (including the AMD) as η_t, then η_t has to fulfill:

$$0.7 \times 16.8 \times \eta_t = 2.5(e^+/e^-) \tag{5}$$

where 0.70 is the capture efficiency of the spent electron's capture system, which is given by the energy spread of the spent electron beam ($\pm 3\%$) caused by the beamstrahlung at the IP; 16.8 e^+/e^- is the yield of positrons per electron at the target with a wiggler of 35 m length and 1.7 T magnetic field and with a thin target of titanium (0.4 radiation length). Hence from (6), the transmission in AMD and PPA should be > 21%.

Given the accelerating gradient and the iris radius, the beam transmission and its transverse performance at the PPA output are dominated by the longitudinal magnetic field Bz of the solenoid surrounding the accelerating structure. By the calculations using the ASTRA-code[10] and PARMELA we obtain the relations of the η_t vs Bz, as listed in Table 3. By this table one can see that to meet $\eta_t > 21\%$, one has to choose Bz ≥ 0.32 T for the PPA. To match the Bz of the PPA with the one at AMD output, the length of the AMD should be 0.59 m according to the adiabatic variation law of the Bz field along the axis as described in formula (1).

Table 3 Beam transmission vs solenoid field

Bz (T)	AMD Length (m)	η_t
0.25	0.77	17.6%
0.32	0.59	21.5%
0.55	0.33	31.7%

4.3 Space-Charge Effects

Taking into account the transmission of about 37.5% in the PPA only (that is the ratio of the number of positrons at the output of the PPA to the number of positrons at the input), then, at the PPA input, one needs $Ne^+ / pulse = 2.8 \times 10^{14}$, and $Ne^+ / bunch = 2.48 \times 10^{11}$ and 1.24×10^{11} for the TESLA versions of Standard-500 and Reduced ε_y-500, respectively. Hence the bunch charges are 40 nC and 20 nC, and the bunch currents (averaged over the RF period of 1.3 GHz defined by the PARMELA) are about 51.0A and 25.5A respectively at the PPA input.

The beam simulation with PARMELA shows that the space-charge effects on the beam performance, with the beam current mentioned above, are negligible due to the large beam emittance and large longitudinal phase spread. If we take into account the electron bunches as well, which are overlapped in

space with the positron bunches at the PPA input, the rejective space-charge effects can be reasonably neglected.

4.4 Beam Loading Effects

1) Single-Bunch Beam Loading Effect

The single-bunch beam loading effect on the energy distribution in a bunch depends on the short-range longitudinal wake field induced by the bunch. By the well-known scaling law:

$$W_l \sim \begin{cases} Ne^+ \\ 1/a^2 \\ \sigma_z^{-1/2} \end{cases}$$

due to the large iris radius (a > 15 mm) and long bunch length ($\sigma_z \approx$ 6-7 mm) at the PPA, one can imagine that W_l is small. By using ABCI[11], we calculated the longitudinal wake W_l and the related loss factor K_l in a cell, as shown in Figure 4,

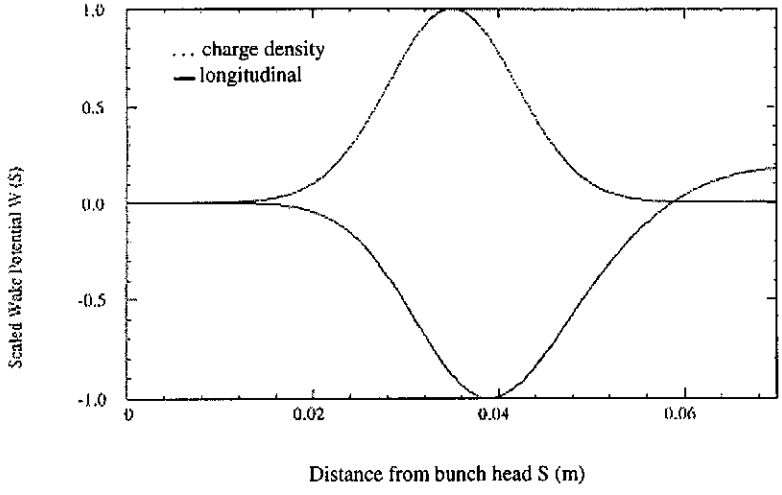

Fig.4 Longitudinal wake field in a cell

with
$$K_l = \frac{1}{q}\int W_l(z)\cdot i_b(z)dz = -0.9992 \text{ V/pC} \qquad (6)$$

Hence the change of the energy distribution due to the wake in a cell, e.g. in the first cell (with max. Ne^+/bunch) of PPA is

$$\Delta W_{\max} = Ne^+ \cdot K_l = -40 \text{ KeV} \qquad (7)$$

This change of the energy distribution in a bunch is negligible compared with the already existing energy spread in a bunch. However it will affect the average energy of a bunch after passing through many cells. By

using the loss factor K_l and taking into account the particle loss in the PPA, the calculated change of the average energy at the PPA output (totally 252 cells) will be a few MeV, which is consistent with the PARMELA simulation, as shown in Table 4.

Table 4 Energy gain with and without beam loading (B.L)

	Average Energy (MeV)	$\varepsilon_{n,x,rms}$ ($\times 10^{-3}$ m)	$\varepsilon_{n,y,rms}$ ($\times 10^{-3}$ m)	Energy Spread (rms)
B.L=0, I=51.0 A	247.7	2.5	2.5	10.6%
B.L≠0, I=51.0 A	241.2	2.5	2.5	9.83%

2) Multi-Bunch (Transient) Beam Loading Effect

As we have mentioned above, during the beam pulse length of 800 μs, the beam power extracted from a section is about 1.21 MW for the first section and 0.65 MW for the following sections. To establish an unloaded gradient of 12 MV/m, each section needs RF power of 6.97 MW. Hence, without compensation for the transient beam loading, the bunch-to-bunch energy change in a section will be about 15%.

A linear amplitude ramp over the pulse length can perfectly compensate the transient beam loading for a constant gradient section with almost constant shunt-impedance per unit length. An rf power of about 20% output from each klystron is reserved for this compensation.

4.5 Parasitic Acceleration of Electron Beam at PPA

As the PPA is optimized to accelerate the positron beam, the electron beam will first be decelerated in the PPA and then accelerated after losing almost all of its energy. Therefore there will be an energy difference between positron and electron beams. The electron beam simulation in the PPA has also been studied by using PARMELA, the beam performance compared with the optimized positron beam are listed in Table 5. The energy difference between positron and electron beam is about 59 MeV.

Table 5 Comparison of positron and electron beam performances at the PPA output

	Energy (MeV)	Transmission	$\varepsilon_{n,x,rms}$ ($\times 10^{-3}$ m)	$\varepsilon_{n,y,rms}$ ($\times 10^{-3}$ m)	Energy Spread (rms)
e^+	247.7	21.5%	2.5	2.5	10.6%
e^-	188.5	14.6%	2.3	2.4	25.9%

At the exit of the PPA, the electrons will be separated from the positrons by using a pair of bending magnets, as shown in Figure 5.

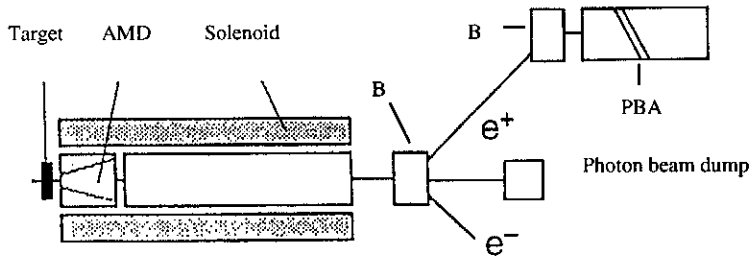

Fig. 5 Layout of Positron and electron beams separation

4.6 Consideration of another option

Another option of the PPA which has a higher gradient of 17 MV/m for the first section (powered by two klystrons of 10 MW each) and a gradient of 12 MV/m for the other sections (powered by one klystron of 10 MW each) has also been studied in order to obtain a smaller rms energy spread and phase spread hence to have more positrons after the energy cutting. First we have shifted the rf phase of the first section to obtain the smaller rms energy spread than the one for the gradient of 12 MV/m for the positron beam at the end of the first section. Then we adjusted the rf phases of the following sections to obtain the average energy of 255.4 MeV and the smaller rms energy spread for the positron beam at the end of PPA. After the energy cutting for $\pm 6.5\%$ energy spread, the remaining positrons are within the phase spread of ± 7.5 degree and the number of positrons is higher than the one at the IP by a factor of 1.93, as compared to 1.9 in case of 12 MV/m.

5 Summary

- A modified cup-like disc-loaded structure for an L-band Positron Pre-Accelerator (PPA, 250 MeV) has been designed. By optimizing the structure geometry and by changing the iris (disc) thickness cell-by-cell in each section, a large iris diameter of > 30 mm and a high shunt-impedance of > 50MΩ/m have been obtained which well meets the requirements of high gradient and large acceptance.

- 12 accelerating sections, with 1.614 m length and 21 cells each, are required to accelerate the positron beam up to about 250 MeV. The total length of the PPA is 19.37 m. Each section needs rf power less than 10 MW which is available and is also used in the TESLA main linac. The accelerating structure is surrounded by a solenoid with a longitudinal magnetic field of 0.32 T to provide the required transverse focusing and beam transmission.

- The beam dynamics in the PPA have been studied for both positrons and parasitic electrons. The space-charge and the single-bunch beam loading effects are not important in the PPA, due to the large beam emittance, energy spread and phase spread at the positron target.

- With an accelerating gradient of 12 MV/m and a solenoid field of 0.32 T, the final PPA-beam performance is listed in Table 6, and shown in Figure 6. We can see that the number of positrons per pulse and the normalized transverse emittance (1.9/1.9$\times 10^{-2}$ m for 100% of the particles) well meet the required Damping Ring acceptance ($\pm 4.8\times 10^{-2}$ m). Regarding the energy spread , we need about ± 16 MeV energy cut (for energy spread of $\pm 6.5\%$) at the position between the two bending magnets, where the dispersion is maximum. The exact energy cut and resulting energy spread needed at the PPA output will be further confirmed by the beam simulation in the PBA to meet the final requirement of the energy spread of $\pm 1\%$ at the PBA output (3.2 GeV). Regarding the phase spread, due to the fact that the positrons in the tail of a bunch have a lower energy than the core positrons (see Fig.6e), this energy cut

also reduces the phase spread. Actually the energy cut simulation indicated that after ± 16 MeV energy cut, the remaining phase spread is about ± 7.0 degree, just as required by the DR, and the remaining number of positrons is about 74%, so that the number of positrons per pulse at the PPA output is a factor of 1.9 higher than at the IP.

Table 6 Positron beam performance at PPA output (after energy cut)

	PPA Design	Required by PBA and DR
Energy (MeV)	248	~250
$\frac{\Delta W}{W}$	$\pm 6.5\%$	$\pm 6.5\ \%$
$\Delta\varphi$	$\pm 7.0^0$	$\pm 7.5^0$
$\varepsilon_x/\varepsilon_y$ (norm.) ($\times 10^{-2}$ m, 100% particles)	1.9 /1.9	≤ 4.8

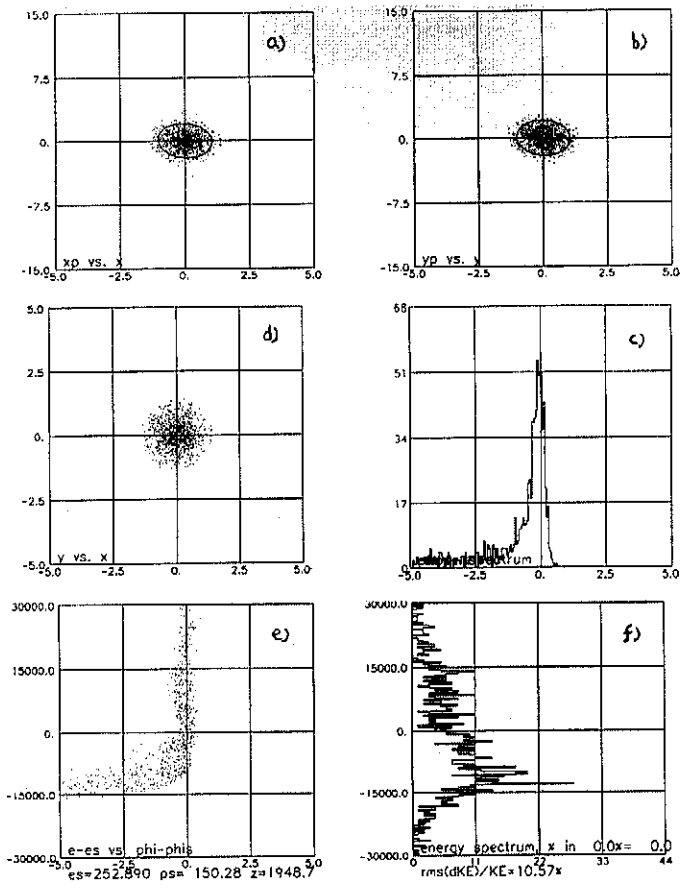

a) x-x' phase space
b) y-y' phase space
c) phase spectrum
d) x vs y beam cross section
e) Δw vs $\Delta\varphi$
f) energy spectrum

Fig. 6 Positron beam performance at the PPA output

Acknowledgments

We would like to thank R.Brinkmann, A.Gamp, N.Holtkamp, V.Paramonov, D.P.Pritzkau, M.Seidel, D.Trines, G.A.Voss and S.Wipf for the helpful discussions and for their interest in this design study.

References

[1] Conceptual Design of a 500 GeV e+e- Linear Collider with Intergrated X-ray Laser Facility (TESLA CDR-500), DESY 1997-048, p403.
[2] K.Floettmann, Investigations Toward the Development of Polarized and Unpolarized High Intensity Positron Sources for Linear Colliders, DESY-93-161, 1993.
[3] TESLA-CDR-500,DESY 1997-048, p430.
[4] TESLA-CDR-500,DESY 1997-048, p290.
[5] TESLA-CDR-500,DESY 1997-048, p431.
[6] TESLA-CDR-500,DESY 1997-048, p614.
[7] MAFIA, The MAFIA collaboration, December 1996.
[8] P.B.Wilson, RF Power Sources for 5TeV-15TeV Linear Colliders, SLAC-PUB-7256, 1996.
[9] PARMELA-code, Lloyd M.Young, LA-UR-96-1835, Revised May 11, 1998.
[10] ASTRA-code, K.Floettmann, private communication.
[11] Y.H.Chin, user's guide for ABCI version 8.8, LBL-35258, 1994.